

NOVEL FLUORESCENT SOFT MATERIAL PREPARED FROM CELLULOSE SOLUTIONS IN ALKALI/UREA AQUEOUS SYSTEM

WENMING ZHANG,* TIANQI WANG,* SHIFENG LI,* KUN CHENG,* SHUANGZHI WEI,*
LING LI,* JIE MENG** and YU ZHAO***

*College of Physics Science and Technology, Hebei University, Baoding 071002, China

**Department of Digestive Medicine, Affiliated Hospital of Hebei University, Baoding 071000, China

***Department of Physical Education, Hebei University, Baoding 071000, China

✉ Corresponding authors: Ling Li, lilingshu@163.com; JieMeng, cenci@163.com; Yu Zhao, zhaoxue1228913@sina.com

Received August 26, 2016

A series of novel cellulose-based hybrid hydrogels were prepared through cellulose and fluorescer Tb³⁺ doped Y₄Si₂O₇N₂ (YT) in NaOH/urea aqueous solution using epichlorohydrin (ECH) as a cross-linker. The structure and properties were characterized by wide-angle X-ray diffraction (XRD), scanning electron microscopy (SEM), FT-IR and fluorescence spectroscopy, as well as by swelling ratio measurements and compression tests. The results revealed that the green fluorescence intensity of the cellulose-based hybrid hydrogels became stronger with an increase of YT contents. The hybrid hydrogels exhibited homogeneous porous structures and the YT particles were tightly embedded in the macroporous cellulose matrix. When the content of YT particles was 0.02 g, the cellulose-based hybrid hydrogels (YTCH3) exhibited stronger fluorescence intensity, higher compressive strength and modulus, and lower swelling ratio.

Keywords: cellulose, hydrogels, compressive strength, swelling ratio, fluorescence intensity, fluorescer

INTRODUCTION

Hydrogels, composite materials that are three-dimensional, hydrophilic, polymeric networks able to absorb large amounts of water or biological fluids, have received increasing attention in recent times. Due to their many favorable properties, such as soft tissue-mimicking consistency, hydrophilicity, high permeability to metabolites and oxygen, and resilience, hydrogels have been considered for a wide variety of applications, such as sensors, tissue engineering, drug-delivery systems, immunoassay, biomedicine *etc.*¹⁻⁸ From the variety of known hydrogels, luminescent bio-based hydrogels not only display visible light under the irradiation of ultraviolet (UV) or near-infrared light (NIR), but also present excellent biomass performance, and have been applied in many fields, such as sensing imaging, for luminescent probes, optical switches *etc.*⁹⁻¹⁵

Rare earth materials are environmentally friendly fluorescent compounds from ores, which are currently widely used in metallurgy,

agriculture, ceramics and the manufacture of new functional materials.¹⁶⁻¹⁹

Lanthanide-doped fluorescer has been extensively applied in chemical and biological sensing systems, and has caused tremendous concern in the past decades.²⁰⁻²² As a result, numerous drawbacks have been overcome, such as quenching luminescence in water and difficult synthesis, making them broadly applicable.²³⁻²⁵ In addition, compared to other fluorescent materials, the unique properties of lanthanide-doped fluorescer include long lifetime, sharp emission peaks, high color purity, and low long-term toxicity.²⁶⁻²⁸ Y₄Si₂O₇N₂:Tb³⁺, a variety of rare earth doped fluorescent materials, exhibits high chemical stability, broad band excitation and good fluorescence characteristics, also, it can be used for white light-emitting diodes.²⁹ So far, reports of fluorescer doped into hydrogels are very scarce. Among the numerous natural macromolecules used for hydrogel formation, cellulose is the most abundant natural polymer available worldwide,

and it can be an alternative resource due to its eco-friendliness, cost-effectiveness, biodegradability and biocompatibility.³⁰⁻³² Zhang *et al.* found that cellulose can be dissolved in an alkali/urea aqueous solution,³³ and quantum dots (QDs)-cellulose hydrogel can be directly fabricated from the cellulose solution.³⁴ However, related studies are very limited. In addition, to the best of our knowledge, there are few studies focused specifically on fluorescer YT-cellulose hybrid hydrogels in alkali/urea systems.

In the present work, we prepared novel hybrid hydrogels based on cellulose by embedding YT into network hydrogels. The incorporation of YT into cellulose can improve the chemical and physical features of the hydrogels. The structure and properties of the prepared hydrogels were characterized by X-ray diffraction, FT-IR spectroscopy, scanning electron microscopy, fluorescence spectroscopy, compression testing and swelling ratio.

EXPERIMENTAL

Materials

Microcrystalline cellulose (cotton linter pulp) was purchased from Shanghai Chemical Co. China. Epichlorohydrin (ECH) was of analytical grade, and was purchased from Shanghai Reagent Chemical Co. China. $Y_4Si_2O_7N_2: Tb^{3+}$ was provided by Lu's group from Hebei University. All other reagents used were of analytical grade and were used without further purification.

Preparation of fluorescent hybrid hydrogels

NaOH (6 g) and urea (4 g) were dissolved in deionized water (86 g) and stirred until well-distributed, then the solution was stored under refrigeration ($-20\text{ }^\circ\text{C}$) for 6 h. Pre-cooled microcrystalline cellulose (4 g) was added into the solution under stirring for 30 min, finally, the cellulose solution was obtained. The cellulose solution (10 g) was transferred to four bottles, which were named as YTCH0, YTCH1, YTCH2 and YTCH3, respectively, corresponding to 0 g, 0.005 g, 0.01 g, 0.02 g of YT content. Epichlorohydrin (ECH) (0.8 g) was added as a cross-linker under stirring for approximately 30 min to yield a homogeneous solution. Then, the cellulose-YT hybrid hydrogels were obtained after reacting at $60\text{ }^\circ\text{C}$ for 1 h.

Characterizations

Swelling ratio measurement of fluorescent hybrid hydrogels

To reach the swelling equilibrium, the samples were nurtured in deionized water at ambient temperature for 24 h. The water absorbency (SR) of the YTCHs was calculated by the following equation:

$$SR = \frac{W_h - W_d}{W_d} \quad (1)$$

where W_d is the dried weight of YTCH and W_h is the wet weight of YTCH hydrogels, respectively.

FT-IR analysis

FT-IR spectra of the dry cellulose fluorescent hybrid hydrogels were recorded using a Fourier Transform Infrared Spectrophotometer (Thermo Nicolet 380). All measurements were carried out by the KBr disk technique within the frequency range of $400\text{--}4000\text{ cm}^{-1}$ in the transmission mode.

Morphology of fluorescent hybrid hydrogels

The fluorescent hybrid hydrogels were first immersed into distilled water to reach equilibrium swelling, and then the swollen hydrogel samples were freeze-dried. Surface and fracture section images of the hydrogels were obtained by field-emission scanning electron microscopy (SEM, Quanta FEG). Specimens were coated with gold for 30 s in SEM coating equipment. The acceleration voltage of SEM was 10 kV.

XRD analysis

Wide-angle X-ray diffraction (XRD) patterns of cellulose and YTCHs were collected on a Philips X'Pert PW-3040 diffractometer (45 KV, 30 mA) with $\text{Cu K}\alpha_1$ radiation.

Optical properties of fluorescent hybrid hydrogels

The fluorescence spectra were recorded on a Hitachi F-4500 fluorescence spectrophotometer at room temperature. YTCH samples were cut into cylinders and placed in a test station. The samples were pre-excited by 365 nm UV for 1 min.

Mechanical properties of fluorescent hybrid hydrogels

The compressive strength of cellulose-based fluorescent hybrid hydrogels was measured on an RGT-5 universal testing machine (Shenzhen Reger Instrument Co, Shenzhen, China) with a crosshead displacement rate of 0.5 mm/min, according to ISO527-3-1995 (E).

RESULTS AND DISCUSSION

Swelling ratios of fluorescent hybrid hydrogels

The swelling ratios of YTCH samples in distilled water are shown in Figure 1. The samples displayed high equilibrium swelling ratios, which further confirmed that the highly hydrophilic groups of cellulose could absorb a great amount of water in the hydrogels. It is worth noting that the swelling ratios of the hydrogels decreased with the increase of YT contents and YTCH3 exhibited the lowest swelling ratio. It was inferred that the fluorescent particles were embedded in the macroporous network of cellulose, which

hindered the penetration of water into the entire hydrogel network.

Morphology analysis of fluorescent hybrid hydrogels

Figure 2 shows the SEM images of YTCH0 (a), YTCH3 (b), and a higher magnification of YTCH3 (c). SEM analysis indicates that pure cellulose hydrogels and cellulose-based fluorescent hybrid hydrogels exhibit a homogeneous micropore structure. The pores of the YTCH0 hydrogel are larger and the cellulose pore wall of the YTCH0 hydrogel is smoother than that of the YTCH3 hydrogel. As shown in Figure 2c, YT particles were immobilized tightly in the membrane of the cellulose pore wall. This may indicate that YT particles and the cellulose solution had good miscibility and the cellulose pore wall effectively prevented the aggregation of YT particles. In addition, the doped YT particles changed the network structure of the cellulose hybrid hydrogels and made the pores smaller,

which was the reason for the low swelling ratio of YTCH3.

XRD analysis of fluorescent hybrid hydrogels

The XRD patterns of YT, YTCH0 and YTCH3 are shown in Figure 3. The YTCH0 and YTCH3 samples displayed the typical amorphous peak at $2\theta=19.5^\circ$, which was assigned to regenerated cellulose (cellulose II). The main diffraction peaks of regenerated cellulose at 12° , 21° and 22° were not observed, demonstrating that chemical crosslinking occurred during the formation of the hydrogel, resulting in the destruction of the initial crystalline structure of cellulose. The sharp peaks of YT showed excellent crystallinity, indicating pure monoclinic phase diffraction peaks of the fluorescer. Interestingly, the special peaks of the fluorescer could be observed in the patterns of YTCH3, indicating that the fluorescer was incorporated successfully into the cellulose matrix and the crystal structure of the fluorescer was well retained in the cellulose hydrogels.

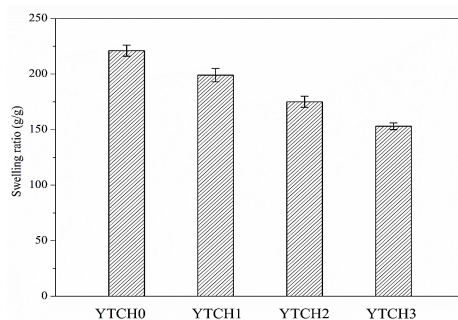


Figure 1: Equilibrium swelling ratio of YTCHs in deionized water

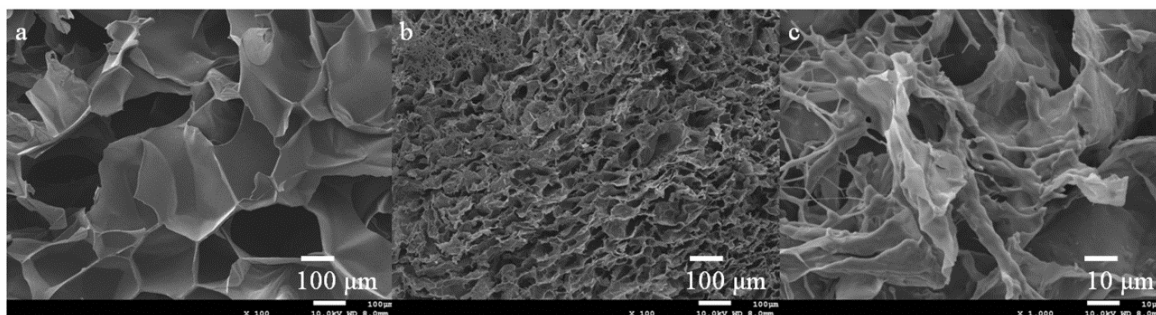


Figure 2: SEM images of YTCH0 (a), YTCH3 (b) and a higher magnification of YTCH3 (c)

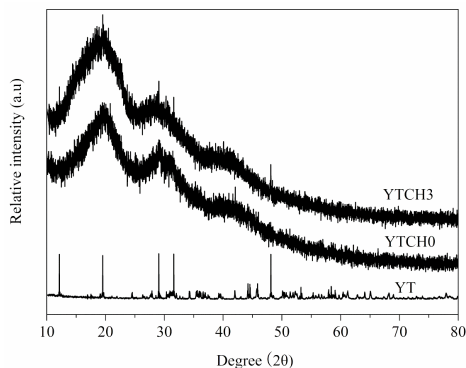


Figure 3: XRD patterns of YT, YTCH0 and YTCH3



Figure 4: Photographs of YTCHs under visible light (a) and UV light of 365 nm (b)

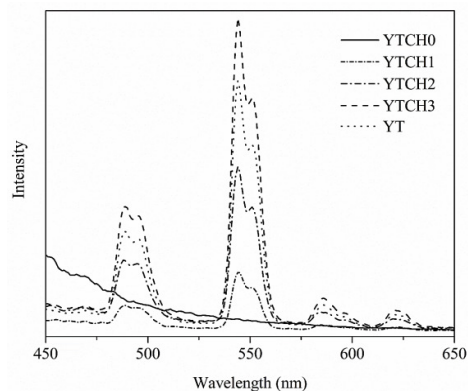


Figure 5: Fluorescence spectra of YTCHs

Optical properties of fluorescent hybrid hydrogels

Photographs of YTCH0, YTCH1, YTCH2 and YTCH3 under visible light (a), and UV light of 365 nm (b) are shown in Figure 4. The YTCH0 hydrogel presented good transparency, while the transparency of YTCH1, YTCH2 and YTCH3 decreased with the increase of YT particles content. This may be due to the fact that the light scattering and reflection of hybrid hydrogels increased when they were doped with a greater amount of YT particles, which resulted in light propagation. As shown in Figure 3b, under UV light, there was no fluorescence in the YTCH0 hydrogel, while green fluorescence was observed clearly and increased with the increase of YT particles content from YTCH1 to YTCH3 hydrogels.

Fluorescence spectra of cellulose fluorescent hybrid hydrogels

Figure 5 shows the fluorescence spectra of YTCHs. It was found that YT and YTCHs exhibited afterglow emission at 489 nm, 495 nm,

544 nm and 551 nm and the emission peaks of hybrid hydrogels were in accordance with those of the fluorescer. Moreover, the intensity of the afterglow enhanced with the increase in the content of YT particles, indicating that cellulose pores played an important role in protecting the structure and fluorescent performance of YT.

Mechanical properties of fluorescent hybrid hydrogels

The compression strength (a) and Young's modulus (b) of YTCHs are shown in Figure 6. YTCH0 exhibited a compressive strength of approximately 20 KPa, whereas the compressive strength of YTCH1, YTCH2 and YTCH3 increased with the increase of YT particles content and YTCH3 showed the highest compressive strength of 62 KPa. This may be because the YT particles adhered to the cellulose matrix, when the cellulose-based hybrid hydrogels were formed, causing a decrease in the pores of the hybrid hydrogels and strengthening of the network structure, which resulted in the reinforcing effect of YTCHs. As shown in Figure

6b, Young's modulus of YTCHs increased significantly from 15.7 KPa to 19.5 KPa. These results indicate that the mechanical properties of the hybrid hydrogels were enhanced by adding YT particles into the cellulose matrix, which is in accordance with the microstructure and fluorescence analyses of YTCHs.

FT-IR analysis of fluorescent hybrid hydrogels

Figure 7 shows the FT-IR spectra of YTCH0 (a) and YTCH3 (b). The absorption bands at 3423 and 2920 cm^{-1} are attributable to the $-\text{OH}$, $-\text{CH}$ or

$-\text{CH}_2$ groups stretching vibration, respectively. The bending vibration of the $\text{H}-\text{O}-\text{H}$ of water absorption, $-\text{CH}_2$, $\text{C}-\text{H}$ groups from cellulose appeared at 1637, 1425, 1317 and 1373 cm^{-1} , respectively. The peaks at 1236, 1164, 1110, 1058 and 897 cm^{-1} can be associated with the $\text{C}-\text{O}-\text{C}$, $\text{C}=\text{O}$, glycosidic bond stretching vibration, respectively.

As may be noted in Figure 7(b), YTCH3 shows a new absorption peak at 549 cm^{-1} with the incorporation of fluorescer, possibly corresponding to the vibration of $\text{Y}-\text{O}$.

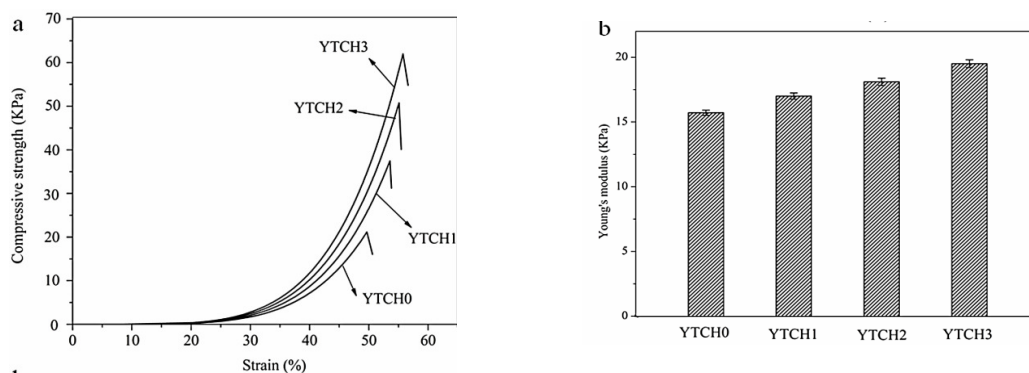


Figure 6: Compression strength (a) and Young's modulus (b) of YTCHs

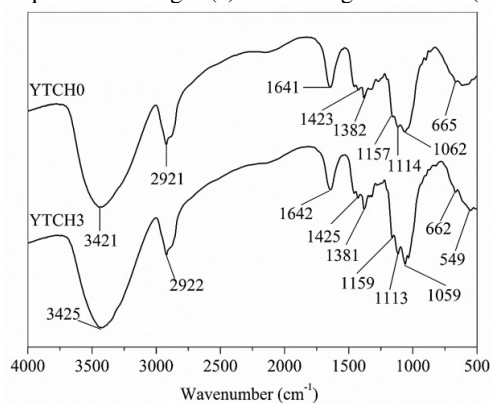


Figure 7: FT-IR spectra of YTCH0 (a) and YTCH3 (b)

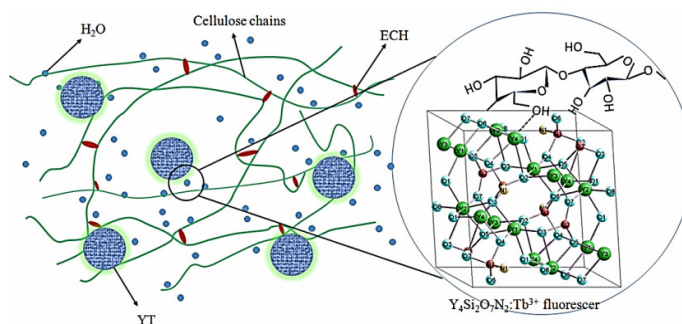


Figure 8: Formation mechanism of YTCHs

These results further indicate that YT was successfully incorporated into the cellulose matrix, which is consistent with the XRD and SEM results.

Formation mechanism of fluorescent hybrid hydrogels

Respecting the above-mentioned results, a mechanism of YTCH formation was proposed, as shown in Figure 8. The cellulose fluorescent hybrid hydrogels were synthesized by cellulose and $Y_4Si_2O_7N_2:Tb^{3+}$ (YT) in NaOH/urea solution, using ECH as a cross-linker. The fluorescer YT particles were immobilized in the cellulose matrix through physical interaction between cellulose and YT, because of the strong affinity of cellulose for inorganic particles, including hydrogen bonds and van der Waals forces. In addition, the network structure of the cellulose matrix provided not only cavities to fasten the YT particles, but also pore walls for their support, serving as a hull to protect the structure and character of the YT.

CONCLUSION

A series of novel hybrid hydrogels containing cellulose and various fluorescer $Y_4Si_2O_7N_2:Tb^{3+}$ (YT) content were prepared using epichlorohydrin (ECH) as a cross-linker. The YT particles were successfully embedded in the cellulose matrix and dispersed homogeneously. The original crystal structure and properties of YT particles were maintained in the hybrid hydrogels, maintaining a strong green emission under UV light. The fluorescence intensity, compression strength and Young's modulus enhanced and the swelling ratio of the hybrid hydrogels in distilled water decreased with an increase of YT particles content. The network structure of the cellulose matrix provided not only cavities to fasten the YT particles, but also pore walls to support them, acting as a hull to protect the structure and character of YT.

ACKNOWLEDGEMENTS: We gratefully acknowledge the financial support from the following sources: National Natural Science Foundation of China (NSFC) (Grants 21201053, 51607054), Hebei Province Natural Science Foundation (F2014201078, A2015201050), Hebei Province Department of Education (Key Project ZD2016055), Outstanding Youth Fund of Hebei University (2015JQ02), Post-graduate's Innovation Project of Hebei University

(X2016065, X2016066) and The Second Batch of Young Talent of Hebei Province.

REFERENCES

- W. E. Hennink and C. F. Van Nostrum, *Adv. Drug Deliv. Rev.*, **54**, 13 (2002).
- A. S. Hoffman, *Adv. Drug Deliv. Rev.*, **54**, 3 (2002).
- H. Chen and A. Q. Wang, *J. Hazard. Mater.*, **165**, 223 (2009).
- D. Buenger, F. Topuz and J. Groll, *Prog. Polym. Sci.*, **37**, 1678 (2012).
- K. T. Nguyen and J. L. West, *Biomaterials*, **23**, 4307 (2002).
- Y. Qiu and K. Park, *Adv. Drug Deliv. Rev.*, **53**, 321 (2001).
- A. Y. Rubin, V. I. Dyukova, E. I. Dementieva, A. A. Stomakhin, V. A. Nesmeyanov *et al.*, *Anal. Biochem.*, **340**, 317 (2005).
- N. A. Peppas, J. Z. Hilt, A. Khademhosseini and R. Langer, *Adv. Mater.*, **18**, 1345 (2006).
- C. L. Tan and Q. M. Wang, *J. Fluoresc.*, **22**, 1581 (2012).
- L. Xiong, J. Feng, R. Hu, S. Q. Wang, S. Y. Li *et al.*, *Anal. Chem.*, **85**, 4113 (2013).
- L. G. Zhang, C. L. Tan, Q. M. Wang and C. C. Zhang, *Photochem. Photobiol.*, **87**, 1036 (2011).
- Y. H. Zheng, S. T. Pang, Z. Zhou, Q. M. Wang, C. L. Tan *et al.*, *J. Cluster Sci.*, **24**, 449 (2013).
- S. M. Borisov, A. S. Vasylevska, C. Krause and O. S. Wolfbeis, *Adv. Funct. Mater.*, **16**, 1536 (2006).
- L. Maggini, M. J. Liu, Y. Ishida and D. Bonifazi, *Adv. Mater.*, **25**, 2462 (2014).
- Z. Zhou and Q. M. Wang, *Sens. Actuators. B*, **173**, 833 (2012).
- C. X. Li and J. Lin, *J. Mater. Chem.*, **20**, 6831 (2010).
- Y. F. Ding, C. Wen, P. Hodgson and Y. C. Li, *J. Mater. Chem. B.*, **2**, 1912 (2014).
- S. Bingham and W. A. Daoud, *J. Mater. Chem.*, **21**, 2041 (2011).
- S. V. Eliseeva and J.-C. G. Bünzli, *New J. Chem.*, **35**, 1165 (2011).
- C. P. McCoy, F. Stomeo, S. E. Plush and T. Gunnlaugsson, *Chem. Mater.*, **18**, 4336 (2006).
- F. Camerel, L. Bonardi, M. Schmutz and R. Ziessel, *J. Am. Chem. Soc.*, **128**, 4548 (2006).
- F. Fages, *Angew. Chem. Int. Ed.*, **45**, 1680 (2006).
- K. Binnemans and C. Görller-Walrand, *Chem. Rev.*, **102**, 2303 (2002).
- S. H. Seo and J. Y. Chang, *Chem. Mater.*, **17**, 3249 (2005).
- S. Mukhopadhyay, G. Krishnamoorthy and U. Maitra, *J. Phys. Chem. B.*, **107**, 2189 (2003).
- M. Mitsuishi, S. Kikuchi, T. Miyashita and Y. Amao, *J. Mater. Chem.*, **13**, 2875 (2003).
- J.-C. G. Bünzli and C. Piguet, *Chem. Soc. Rev.*, **34**, 1048 (2005).
- J.-C. G. Bünzli, *Acc. Chem. Res.*, **39**, 53 (2006).

²⁹ F. C. Lu, X. P. Song and Q. L. Liu, *J. Optical Mater.*, **33**, 91 (2010).

³⁰ T. Tominaga, V. R. Tirumala, S. Lee, E. K. Lin, J. P. Gong *et al.*, *J. Phys. Chem. B*, **112**, 3903 (2008).

³¹ J. Schurz, *Prog. Polym. Sci.*, **24**, 481 (1999).

³² S. J. Eichhorn, R. J. Young and G. R. Davies, *Biomacromolecules*, **6**, 507 (2005).

³³ J. Cai and L. N. Zhang, *Macromol. Biosci.*, **5**, 539 (2005).

³⁴ C. Y. Chang, J. Peng, L. N. Zhang and D. W. Pang, *J. Mater. Chem.*, **19**, 7771 (2009).